

# Logic Synthesis Optimization with Predictive Self-Supervision via Causal Transformers

Raika Karimi  
raika.karimi@huawei.com  
Huawei Noah's Ark Lab  
Toronto, Canada

Xing Li  
li.xing2@huawei.com  
Huawei Noah's Ark Lab  
Hong Kong, China

Faezeh Faez  
faezeh.faez@huawei.com  
Huawei Noah's Ark Lab  
Toronto, Canada

Lei Chen  
lc.leichen@huawei.com  
Huawei Noah's Ark Lab  
Hong Kong, China

Yingxue Zhang  
yingxue.zhang@huawei.com  
Huawei Noah's Ark Lab  
Toronto, Canada

Mingxuan Yuan  
yuan.mingxuan@huawei.com  
Huawei Noah's Ark Lab  
Hong Kong, China

Mahdi Biparva  
mahdi.biparva@huawei.com  
Huawei Noah's Ark Lab  
Toronto, Canada

## ABSTRACT

Contemporary hardware design benefits from the abstraction provided by high-level logic gates, streamlining the implementation of logic circuits. Logic Synthesis Optimization (LSO) operates at one level of abstraction within the Electronic Design Automation (EDA) workflow, targeting improvements in logic circuits with respect to performance metrics such as size and speed in the final layout. Recent trends in the field show a growing interest in leveraging Machine Learning (ML) for EDA, notably through ML-guided logic synthesis utilizing policy-based Reinforcement Learning (RL) methods. Despite these advancements, existing models face challenges such as overfitting and limited generalization, attributed to constrained public circuits and the expressiveness limitations of graph encoders. To address these hurdles, and tackle data scarcity issues, we introduce LSOformer, a novel approach harnessing Autoregressive transformer models and predictive SSL to predict the trajectory of Quality of Results (QoR). LSOformer integrates cross-attention modules to merge insights from circuit graphs and optimization sequences, thereby enhancing prediction accuracy for QoR metrics. Experimental studies validate the effectiveness of LSOformer, showcasing its superior performance over baseline architectures in QoR prediction tasks, where it achieves improvements of 5.74%, 4.35%, and 17.06% on the EPFL, OABCD, and proprietary circuits datasets, respectively, in inductive setup.

## CCS CONCEPTS

- **Hardware** → **Electronic design automation (EDA); Logic synthesis; Computing methodologies** → **Machine learning**

Permission to make digital or hard copies of all or part of this work for personal or classroom use is granted without fee provided that copies are not made or distributed for profit or commercial advantage and that copies bear this notice and the full citation on the first page. Copyrights for components of this work owned by others than the author(s) must be honored. Abstracting with credit is permitted. To copy otherwise, or republish, to post on servers or to redistribute to lists, requires prior specific permission and/or a fee. Request permissions from permissions@acm.org.

DAC, June 22–25, 2025, San Francisco, CA

© 2018 Copyright held by the owner/author(s). Publication rights licensed to ACM. ACM ISBN 978-1-4503-XXXX-X/18/06...\$15.00  
https://doi.org/XXXXXXX.XXXXXXX

## KEYWORDS

Logic Synthesis Optimization, Graph Representation Learning, Predictive Self-supervised Learning, Transformers

## ACM Reference Format:

Raika Karimi, Faezeh Faez, Yingxue Zhang, Xing Li, Lei Chen, Mingxuan Yuan, and Mahdi Biparva. 2018. Logic Synthesis Optimization with Predictive Self-Supervision via Causal Transformers. In *Proceedings of The Design Automation Conference (DAC)*. ACM, New York, NY, USA, 8 pages. <https://doi.org/XXXXXXX.XXXXXXX>

## 1 INTRODUCTION

In contemporary hardware design, the creation of hardware devices is facilitated by the abstraction provided by high-level logic gates, liberating designers from the intricacies of Integrated Circuit (IC) implementation. During the IC fabrication process, the conceptual designs are translated into tangible layouts with the aid of Electronic Design Automation (EDA) tools. In essence, EDA tools afford designers the opportunity to focus exclusively on the functional aspects of their designs at a high-level by employing hardware description languages (HDL) like Verilog.

logic synthesis optimization (LSO) in which a logic circuit is transformed into a functionally equivalent and optimized representation is a part of EDA workflow [26]. In LSO, a sequence of optimization transformations supported by academia and industry [4] and named **recipe** are applied to logic-level circuit designs to optimize performance criteria such as size and speed, named Quality of Results (QoR), in the final IC.

Due to high latency and long running time of EDA tools, there is a huge surge of interest to use Machine Learning (ML) for EDA [11, 13, 16, 28, 39], specifically ML-guided logic synthesis [16], [38]. In addressing this, logic synthesis designers frequently employ policy-based Reinforcement Learning (RL) methods to identify optimal recipes [14]. Given the time-intensive nature of searches, leveraging pre-trained policy functions can expedite RL processes [8]. This has introduced a new research challenge: developing ML models that act as policy functions or serve as alternatives to running costly

EDA pipelines, capable of accurately mapping a pair of gate-level circuit representations and a recipe to the final QoR [10].

Most models in this domain represent logic-level circuit designs using the And-Inverter Graph (**AIG**) format [21], which adopts a Directed Acyclic Graph (**DAG**) structure with partially ordered nodes [22]. Significant research efforts have aimed at embedding the inductive bias of DAGs into message-passing graph encoders [29] and graph transformers [20] to enhance model expressiveness. One contribution of our work extends these concepts by generating graph-level representations specifically optimized for AIGs.

The current QoR prediction models often experience overfitting due to a limited number of publicly available circuits used during training, resulting in a lack of generalization, especially when tested on unseen circuits that differ in size and characteristics from the training circuits. Additionally, these models struggle with imbalanced input samples across different modalities; typically, there are more recipe available than AIGs. This disparity can lead to prominent overfitting, particularly due to the low expressiveness of graph encoders, which becomes exacerbated when the model excessively adapts to the encoder part handling recipe.

Self-supervised learning (SSL) has recently emerged as a powerful framework to mitigate data scarcity and address expressiveness limitations in downstream tasks related to LSO [7, 32]. By pre-training circuit encoders and fine-tuning them for specific applications, SSL offers an efficient alternative to conventional data augmentation. Inspired by predictive SSL paradigms [19], this work introduces an auxiliary task that predicts intermediate QoRs, enabling a joint training approach that strengthens the supervisory signal and enhances model learning dynamics.

Existing approaches face a critical limitation in the recipe encoder, which operates in isolation from AIG representations, leading to an inherent information bottleneck. This limitation becomes particularly evident when AIG and recipe embeddings are fused using conventional concatenation methods. This limitation motivated us to develop a decoder-only transformer model for training, employing a joint loss function. As a result, the model contextualizes the embeddings of heuristics using AIG embeddings through a Cross-Attention module, facilitating more effective integration of information.

In summary, we propose the following innovations to address aforementioned drawbacks:

- **Level-wise Graph Pooling:** An efficient graph pooling mechanism tailored for DAG structures that transforms AIG into a sequence of embeddings.
- **QoR Trajectory Prediction:** An auxiliary predictive SSL task designed to predict intermediate QoR for joint training.
- **Causal Transformer:** A decoder-only transformer model that causally predicts QoR based on the recipes and AIGs.
- **Contextualized Fusion:** An efficient mechanism to fuse embeddings of AIGs and recipes using a cross-attention module. This approach contextualizes the embeddings of recipes with AIGs, enabling the model to learn which parts of the graph each heuristic attends to.

Our SOTA model has been tested across multiple datasets, showcasing superior performance in terms of Mean Absolute Percentage

Error (MAPE) when compared to conventional baseline architectures for QoR prediction. Furthermore, our ablation studies justifies that the novel architecture designed for downstream task aligns effectively with predictive SSL tasks. This synergy enhances overall performance beyond that of individual models, also suggesting that the challenges associated with limited datasets have been effectively mitigated through the SSL approach.

## 2 RELATED WORK

Logic synthesis necessitates thorough adjustment of the synthesis optimization procedure, with the QoR contingent upon the optimization sequence applied. Effectively exploring the design space presents a challenge due to the exponential array of potential optimization permutations [12]. Consequently, fast and efficient automation of the optimization procedure becomes imperative [17, 27]. [8, 9, 14, 15, 23, 31] introduce innovative methodologies based on Qlearning-based, Bayesian Optimization, and policy-based RL, which autonomously traverse the optimization space, obviating the need for human intervention.

Several policy-based RL methodologies, such as those discussed in [8, 36, 38], leverage a pre-trained function that correlates initial circuits and recipe with the ultimate QoR. This architecture is split into two primary branches: one for encoding AIGs and another for recipes, along with a fusion branch that maps the embeddings onto the predicted QoR. Similar efforts to forecast QoRs based on initial graphs and recipe are documented in [10, 35–38, 40], where various graph and sequence encoders are explored. Discussions abound concerning the most effective AIG encoders and methods for integrating sequence embeddings with graph embeddings. As a result, improvements in encoder and fusion modules are crucial for enhancing prediction performance. For example, [10] utilizes a GCN to encode graphs and a CNN for recipes, employing both mean and max pooling for graph combination. Meanwhile, [37] employs GraphSage for graph encoding and a transformer for recipe encoding. Similar to one of recent baselines, LOSTIN [35], [38] integrates a Graph Isomorphism Network (GINE) for graph learning with an LSTM for recipe encoding. Additionally, [36] explores various graph encoders, such as PNA and pooling techniques, alongside virtual supernodes in conjunction with hierarchical learning and RL methods. In all aforementioned methods, recipe embeddings and Graph embeddings are fused using concatenation. The MLP decoder has been used to generate the predicted QoR after fusion. However, none of these models utilize an attention mechanism to fuse the two branches.

**SSL for EDA:** Various forms of SSL, including predictive and contrastive approaches, have demonstrated substantial enhancements in tasks within the graph domain [34]. Different SSL protocols can be devised for pre-training or jointly training graph encoders through graph-level pretext tasks [19]. Additionally, SSL provides an alternative to costly data augmentation for AIGs [18], offering a promising method to enhance the expressiveness of AIG encoders and tackle issues related to data scarcity. For instance, [7] employs contrastive learning to pre-train AIG encoders for the Netlist classification task. Similarly, [32] establishes a baseline for contrastive learning in netlist representation.

**Table 1: Overall notation table of the main symbols in the paper.**

basic notations	
$N$	The number of nodes.
$E$	The number of edges.
$D$	The maximum depth of the AIG
$C$	The number of available heuristics
$R$	The number of available recipes
$M$	The maximum length of recipe
$\hat{y}$	The prediction of final ground truth QoR
$y_k$	The ground truth QoR of $k^{th}$ step
Sets	
$H$	The set of node embeddings
$H^l$	The set of embeddings for nodes located at $l^{th}$ level of AIG.
$\mathcal{G}$	AIG Graph
$\mathcal{V}$	The set of vertices.
$\mathcal{E}$	The set of edges
$X^v$	The node features.
$X_{type}^v$	The node type
$X_{inverted}^v$	The number of inverted inputs for each node
$\mathcal{T}$	Set of Available Heuristics
$\mathcal{R}$	The set of recipes
$u_i$	$i^{th}$ heuristic within a given recipe
$d_h$	the node embedding dimension.
Sequences	
$\tilde{H}$	Sequence representation of AIG
$r_i$	$i^{th}$ recipe
$\tilde{r}_i$	Sequence of embeddings for $i^{th}$ recipe
$z_i$	Sequence of positionally encoded embeddings for $i^{th}$ recipe
$\tilde{z}_i$	Contextualized heuristics' embeddings
$\tilde{h}^i$	Output sequence of embeddings for input AIG and $i^{th}$ recipe
Matrices and Vectors	
$\tilde{u}_i$	Embedding vector for $i^{th}$ heuristic of a given recipe
$\tilde{h}_i$	$i^{th}$ node embedding
$\tilde{M}$	Upper triangular mask matrix
$\tilde{h}_l$	The embedding of $l^{th}$ level of AIG
Learnable Parameters and functions	
$\theta$	The weight parameters of the encoder.
$\gamma$	The weight parameters of the decoder.

The application of predictive SSL to enhance the expressiveness of transformer-based encoders constitutes a dynamic area of research. For example, [25] demonstrates the use of motif prediction to augment the capabilities of graph transformer encoders. In the domain of sequence processing, researchers employ causal transformers with predictive SSL to enhance their expressiveness [24]. Additionally, next-token prediction exemplifies the use of causal pre-training, which substantially improves the effectiveness of conventional transformers [30].

### 3 METHODOLOGY

In this section, we formalize and describe the Logic Synthesis Optimization (LSO) problem. Next, we present the LSOformer pipeline, specifically designed for LSO, which features a novel architecture tailored for the QoR prediction task. Then, we introduce a Self-Supervised Learning (SSL) auxiliary task aiming at predicting the trajectory of the QoRs given recipe and And-Inverter Graphs (AIG) graphs.

#### 3.1 Problem Definition

The logic-level designs stored in BENCH format are first converted into AIGs, a format initially proposed in [6] for representing logic circuits. An AIG is a type of Directed Acyclic Graph (DAG) [21], characterized by nodes representing 2-input AND functions and

edges signifying either NOT or buffer functions [3]. This structure simplifies the representation and manipulation of boolean functions, facilitating various logic synthesis and optimization tasks.

Consequently, the input AIGs are transformed into attributed directed acyclic graphs (DAGs)  $\mathcal{G} = (\mathcal{V}, \mathcal{E}, \mathcal{X}^v)$ , comprising  $N$  nodes and  $E = |\mathcal{E}|$  directed edges. Node features  $\mathcal{X}^v$  are categorized into two types:  $X_{type}^v \in \{0, 1, 2\}$  and  $X_{inverted}^v \in \{0, 1, 2\}$ . These features represent the classification of nodes (input, output, or intermediate) and the count of inverted predecessors for each gate, respectively. The set of recipe, denoted as  $\mathcal{R} = \{r_1, r_2, \dots, r_R\}$ , comprises  $R$  recipes, each containing  $M$  sequentially ordered heuristics, selected from a set  $\mathcal{T} = \{t_1, t_2, \dots, t_C\}$ , which consists of  $C$  types of heuristics. Each element in  $\mathcal{T}$  is an optimizer.

#### 3.2 Task Definition

**Technology Mapping:** The process involves transforming a network of technology-independent logic gates into a network consisting of logic cells tailored to the layout of a target integrated circuit (IC), such as a Field-Programmable Gate Array (FPGA). The metrics such as delay, area, space can be measured after this step.

**Ground Truth Generation:** In the EDA workflow, we can optimize logic-level circuits modeled by AIG graphs  $\mathcal{G}$  given the recipe through the time consuming tools like ABC. After sequentially applying the  $i^{th}$  heuristic and optimizing the logic-level representation, technology mapping is then applied to map the optimized version, with the ground truth QoR after each step shown by  $y^i$ . The final QoR after  $M^{th}$  heuristics, named  $y$ , is the ground truth of the model that our proposed model is expected to predict given the input AIGs and recipe during inference mode.

**3.2.1 Self-Supervised Learning Auxiliary task.** As an auxiliary task helping the model during training, we train the model to predict the trajectory of QoR evolution. To achieve this, the model step by step predicts all  $M$  intermediate QoRs in a causal manner. For predicting the  $i^{th}$  QoR, the model takes as input all heuristics before the  $i^{th}$  step,  $(r_1, r_2, \dots, r_i)$ . This predictive SSL task by itself is aligned with architecture of our transformer decoder to help model benefits from extra information within intermediate steps.

**3.2.2 Final QoR prediction.** The QoR prediction task aims to find the learnable function  $f_y$  that maps a pair of recipe and AIG graph,  $(\mathcal{G}, r_i)$  to a numerical value  $\hat{y}$  which is a prediction of final ground truth QoR such as delay and area. More specifically, the task is as follows:

$$\hat{y} = f_y(\mathcal{G}, r_i) \quad (1)$$

The final loss which is Mean Squared Error is defined as follows:

$$\text{loss} = \sum_{k=1}^M \text{MSE}(\hat{y}_k, y_k) \quad (2)$$

Where  $y_k$  represents the ground truth QoR of  $k^{th}$  step.

#### 3.3 Architecture

The architecture of our system consists of three main components: the graph encoder, the recipe encoder, and the fusion mechanism

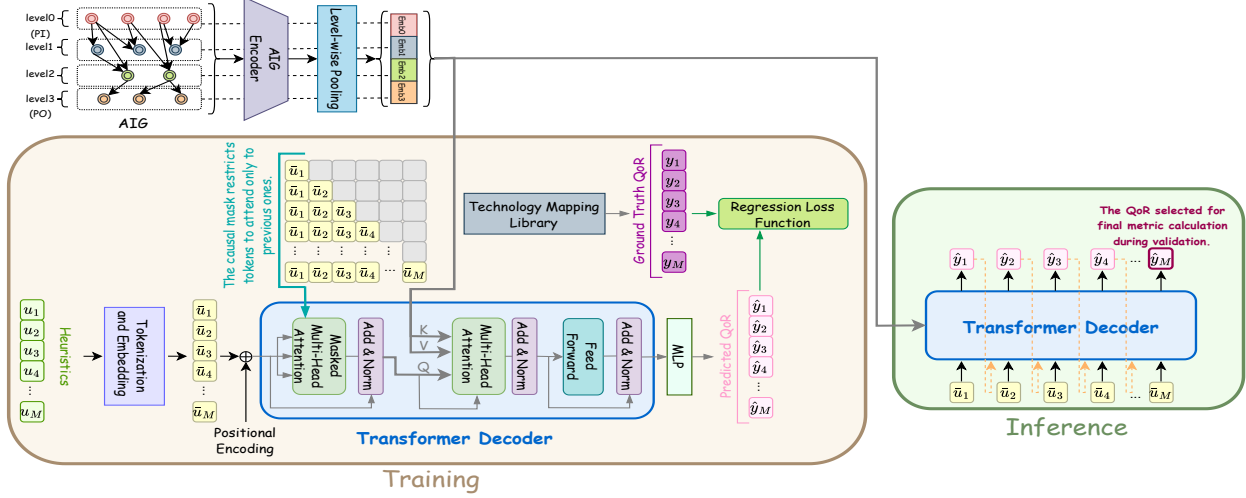


Figure 1: Schematic overview of the LSOformer architecture during training and inference modes.

coupled with the decoder. The novelty of our work primarily lies in the enhancements to the decoding process as well as modifications to the other components. These innovations are detailed below, emphasizing the unique aspects of our approach within each block.

**3.3.1 Graph Encoder.** In the AIG segment, we employ a graph encoder  $\mathcal{E}_\theta$  based on the following formulation:

$$\mathbf{H} = \mathcal{E}_\theta(\mathcal{G}) \quad (3)$$

Here,  $\mathbf{H} = \{h_1, h_2, \dots, h_N\}$  represents the set of node embeddings and  $h_i \in \mathbb{R}^{d_h}$  is  $i^{th}$  node embedding. Similar to the approach used in OpenABC [10], we utilize a Graph Convolutional Neural Network (GCN) with the same node embedding approach to encode the AIGs.

**3.3.2 Level-wise Node Pooling.** Although the GCNs can encode graphs properly, they are unable to particularly incorporate the inductive bias of DAGs. To benefit from this bias to improve the graph representation learner, we propose an unique pooling mechanism called level-wise pooling.

Similar to the work proposed in [20] the depth of a node  $v$  is calculated through the function  $depth(v)$  because of the partial order intrinsic to the DAG. The set of node embeddings can be partitioned based on the depth of the each node as follows:

$$\mathbf{H} = \{\mathbf{H}^0, \mathbf{H}^1, \dots, \mathbf{H}^D\} \quad (4)$$

Where  $\mathbf{H}^l$  represents the set of embeddings for nodes located at  $l^{th}$  level of AIG. Finally, the AIG graph is represented as a sequence for the decoder layer described in the next section. The sequence is derived according to the combination of mean and max poolings as follows:

$$\bar{\mathbf{H}} = (\bar{h}_0, \bar{h}_1, \dots, \bar{h}_D), \quad \bar{h}_l = \text{POOL}_{\text{level}}(\mathbf{H}^l) \quad (5)$$

where  $\bar{\mathbf{H}}$  is the sequence of representation of DAG and  $\bar{h}_l \in \mathbb{R}^{2 \times d_h}$  is the embedding of  $l^{th}$  level of AIG. The  $\text{POOL}_{\text{level}}$  is the concatenation of mean and max poolings.

**3.3.3 Heuristic Tokenization and Embedding.** Each recipe, denoted as  $r_i = (u_1, u_2, \dots, u_M)$ , where each  $u_j \in \mathcal{T}$  represents the  $j$ -th heuristic within the recipe, is tokenized using a one-hot vector of length  $C$ . A lookup table is utilized to generate learned embeddings to convert the input tokens to vectors  $\bar{u}_i \in \mathbb{R}^{2 \times d_h}$  within the sequence of embeddings  $\bar{r}_i = (\bar{u}_1, \bar{u}_2, \dots, \bar{u}_M)$ .

**3.3.4 Transformer Decoder.** Once the recipes are embedded and the AIG is converted to a sequence, inspired by Machine Translation models [30], we propose a sequence to sequence alignment module using only transformer decoder module to fuse the AIG sequence with heuristics' embeddings. In other words, this transformer module maps AIG sequence and heuristics' embeddings to the trajectory of QoRs in causal manner. More specifically:

$$\hat{\mathbf{Y}} = \text{Transformer}(\bar{\mathbf{H}}, \bar{r}_i) \quad (6)$$

$$\hat{\mathbf{Y}} = (\hat{y}_1, \dots, \hat{y}_M) \quad (7)$$

where  $\hat{\mathbf{Y}}$  consists of the QoRs of the trajectory. Our transformer decoder containing 6 main components is designed and formulated as follows:

**Positional Encoding:** Sine/Cosine positional encoding (PE) is added to the sequence of heuristics embeddings element-wise as

**Table 2: Performance comparison of delay and area prediction models across datasets, evaluated using MAPE (Avg.  $\pm$  Std.) (%).**

Architecture	IP-Inductive						Recipe-Inductive					
	EPFL		OABCD		PD		EPFL		OABCD		PD	
	delay	area	delay	area	delay	area	delay	area	delay	area	delay	area
OpenABC (Baseline)	4.18 $\pm$ 0.07	2.46 $\pm$ 0.03	23.66 $\pm$ 0.19	2.71 $\pm$ 0.02	15.88 $\pm$ 0.41	3.57 $\pm$ 0.10	5.35 $\pm$ 0.04	2.74 $\pm$ 0.01	16.79 $\pm$ 0.08	2.72 $\pm$ 0.01	16.69 $\pm$ 0.4	2.04 $\pm$ 0.01
LOSTIN (GIN + LSTM) [35]	3.96 $\pm$ 0.02	2.30 $\pm$ 0.01	24.61 $\pm$ 0.03	2.35 $\pm$ 0.07	16.76 $\pm$ 0.13	3.46 $\pm$ 0.17	5.14 $\pm$ 0.04	2.73 $\pm$ 0.04	17.47 $\pm$ 0.04	1.77 $\pm$ 0.03	17.61 $\pm$ 0.07	2.03 $\pm$ 0.08
(GraphSage + Transformer) [37]	3.96 $\pm$ 0.02	2.39 $\pm$ 0.00	24.58 $\pm$ 0.13	3.77 $\pm$ 0.00	17.09 $\pm$ 0.08	3.81 $\pm$ 0.05	5.79 $\pm$ 0.02	2.96 $\pm$ 0.00	18.33 $\pm$ 0.60	3.4 $\pm$ 0.06	18.04 $\pm$ 0.02	2.43 $\pm$ 0.04
GNN-H [36]	3.96 $\pm$ 0.03	2.34 $\pm$ 0.02	24.31 $\pm$ 0.27	2.33 $\pm$ 0.06	16.80 $\pm$ 0.06	3.59 $\pm$ 0.12	5.79 $\pm$ 0.01	2.61 $\pm$ 0.06	16.41 $\pm$ 0.40	1.58 $\pm$ 0.02	17.52 $\pm$ 0.05	2.15 $\pm$ 0.01
LSOformer (ours)	<b>3.94 <math>\pm</math> 0.02</b>	<b>2.24 <math>\pm</math> 0.02</b>	<b>22.63 <math>\pm</math> 0.04</b>	<b>2.34 <math>\pm</math> 0.05</b>	<b>13.17 <math>\pm</math> 0.28</b>	<b>3.43 <math>\pm</math> 0.05</b>	<b>4.74 <math>\pm</math> 0.01</b>	<b>2.45 <math>\pm</math> 0.03</b>	<b>16.39 <math>\pm</math> 0.16</b>	<b>1.21 <math>\pm</math> 0.03</b>	<b>14.55 <math>\pm</math> 0.02</b>	<b>1.92 <math>\pm</math> 0.03</b>
Improvement % vs Baseline	5.74% $\uparrow$	8.94% $\uparrow$	4.35% $\uparrow$	13.65% $\uparrow$	17.06% $\uparrow$	3.92% $\uparrow$	11.40% $\uparrow$	10.58% $\uparrow$	2.38% $\uparrow$	55.5% $\uparrow$	12.82% $\uparrow$	5.88% $\uparrow$

follows:

$$PE_{(m,2k)} = \sin\left(\frac{m}{10000k/d_h}\right) \quad (8)$$

$$PE_{(m,2k+1)} = \cos\left(\frac{m}{10000k/d_h}\right) \quad (9)$$

$$z_i = \bar{r}_i + PE \quad (10)$$

Where  $z_i$  is the sequence of positionally encoded embeddings of Optimizers.

**Masked Multi-Head Self-Attention:** If  $Q = z_i W_q \in \mathbb{R}^{M \times 2d_h}$ ,  $K = z_i W_k \in \mathbb{R}^{M \times 2d_h}$ , and  $V = z_i W_v \in \mathbb{R}^{M \times 2d_h}$  are the query, key, and value matrices, the contextualized heuristics' embedding ( $\bar{z}_i$ ) is derived as follows:

$$\bar{z}_i = \text{Attention}(Q, K, V) = \text{softmax}\left(\frac{QK^T}{\sqrt{d_k}} + \bar{M}\right)V \quad (11)$$

The mask  $\bar{M}$  is typically an upper triangular matrix with zeros on and below the diagonal and  $-\infty$  above the diagonal for each sequence in the batch. This structure effectively imposes causality and ensures that each position in the sequence can only attend to itself and previous positions, not to any future positions.

**Cross-Attention:** This module computes the attention weights between the element of AIG sequence and contextualized heuristics' embeddings. Finally, a Feed-Forward layer (FFN) with Relu function is applied element-wise to the sequence.

$$\tilde{h}^i = \text{FFN}(\text{MultiHeadAttention}(\bar{z}_i, \bar{H}, \bar{H})) \quad (12)$$

Where  $\tilde{h}^i = (\tilde{u}_1, \tilde{u}_2, \dots, \tilde{u}_M)$  is the output sequence of embeddings for input AIG and  $i^{th}$  recipe;  $\tilde{u}_i \in \mathbb{R}^{2 \times d_h}$  represents generated embedding corresponding to  $i^{th}$  QoR.

**Add & Norm:** Each sub-layer (self-attention and feed-forward network) includes a residual connection followed by layer normalization:

$$\text{LayerNorm}(x + \text{Sublayer}(x)) \quad (13)$$

**MLP Regressor:** Once the embeddings for each QoR has been generated sequentially, we use a MLP module to map the embeddings to final QoR as follows:

$$\hat{y}_i = \text{MLP}(\tilde{h}^i) \quad (14)$$

## 4 EXPERIMENTAL EVALUATION

In this section, we have structured experiments to robustly validate the three main contributions outlined in this work. Following the experimental design, we assess the performance of the proposed architecture across various setups and scenarios, providing a comprehensive evaluation of its effectiveness and adaptability in handling different computational challenges.

### 4.1 Tools

Commercial EDA tools offer standardized operating systems [5], whereas the academic, open-source tool ABC [5] provides specialized heuristic commands for circuit optimization. We employ OpenROAD v1.0 EDA [1] for logic synthesis, with Yosys [33], version 0.9, serving as the frontend engine. Yosys works in collaboration with ABC to carry out post-technology mapping and generate a minimized logic circuit specifically optimized for the final QoR. Post-technology mapping, the area and delay of these designs are evaluated using the NanGate 45nm technology library and the 5K\_heavy wireload model. Furthermore, we utilize PyTorch v1.13 and PyTorch Geometric v2.2.0 to generate AIGs.

### 4.2 Datasets

Three datasets were employed for the experiments, each comprising a collection of circuit designs beside a set of recipe. Since each dataset is used in different studies, we chose not to combine them to simplify comparisons with baseline methods. Additionally, we report performance metrics individually for each dataset. Logic-level circuit designs in the datasets are referred to as Intellectual Property (IP). A consistent set of 1500 unique recipes borrowed from [10] was applied across all datasets. Each recipe was constructed utilizing seven primary heuristics and their associated flags from the ABC toolkit. These heuristics include Balance, Rewrite (rw, rw -z), Refactor (rf, rf -z), and Re-substitution (rs, rs -z).

**EPFL:** Introduced in 2015, the EPFL Combinational Benchmark Suite comprises combinational circuits specifically designed to test

**Table 3: Statistics for benchmark datasets.**

Dataset	EPFL	OABCD	PD
Number of Circuits	15	29	118
Avg # Nodes	7629.25	12092.25	21746.99
Avg # Edges	31035.46	63640.44	40436.10
Avg Depth	1835.8	65.55	56.19
Avg PI	224.75	3118.96	1095.41
Avg PO	143.05	2803.04	867.05

**Table 4: Ablation study on Recipe Encoder (Recipe Enc.) and AIG Encoder (AIG Enc.) using the Freeze Probing setup, evaluated with MAPE.**

Pre-text task setup	QoR Prediction	Frozen GE	Frozen RE	EPFL	OABCD
Random Freeze	✗	✓	✓	5.05	26.74
Random AIG Enc.	✓	✓	✗	4.32	24.37
Random recipe Enc.	✓	✗	✓	4.51	26.13
Freezed LSOformer	✓	✗	✗	3.98	23.5
Supervised baseline	✗	✗	✗	4.26	23.58
Supervised LSOformer	✗	✗	✗	3.94	22.58

the capabilities of modern logic optimization tools [2]. This benchmark suite has been complemented by an open-source leaderboard, which aims to establish a new comparative standard within the logic optimization and synthesis community. The suite is categorized into arithmetic, random/control, and MtM circuits, with each circuit available in multiple formats including Verilog, VHDL, BLIF, and AIG.

**Open ABC Dataset (OABCD):** This dataset comprises 29 circuits followed by a LSO pipeline. The pipeline, as proposed in [10], features an end-to-end preprocessing system designed to handle and execute three regression-based downstream tasks, each dependent on the stage of post-technology mapping. Additionally, the baseline pipeline includes a classification task aimed at evaluating the efficacy of the graph encoder in distinguishing between graphs derived from different Circuits.

**Proprietary Dataset (PD):** This dataset includes 118 internal circuits, with the number of nodes per circuit approximately varying from 80 to 40,000. Additionally, detailed statistics for the number of nodes, depth, number of input nodes (PI), and number of output nodes (PO) in all datasets are provided in Table 3.

### 4.3 Experimental Protocol

The efficacy of our model is assessed under both transductive and inductive settings to demonstrate its superiority over competing architectures. The dataset is split into training and validation sets with ratios of 0.66 and 0.33, respectively, for both setups. Additionally, zero-mean normalization is applied to normalize the final QoRs. Additionally, intermediate QoRs are normalized using the mean and standard deviation derived from the final QoRs. In the ablation study, we focus exclusively on the inductive setting, which presents the most challenging scenario for the LSO problem. In these experiments, given the challenges associated with predicting timing, delay are selected as the target variable for QoR prediction.

**Table 5: Ablation study on the decoder and SSL auxiliary task, evaluated with the MAPE metric. P.Q.T. stands for Predicting QoR trajectory.**

Setup name	P.Q.T.	Transformer decoder	EPFL	OABCD
OpenABC (Baseline)	✗	✗	4.26	23.58
OpenABC + SSL	✓	✗	4.16	26.48
Transformer Decoder	✗	✓	4.01	24.62
LSOformer	✓	✓	3.94	22.58

**Table 6: Ablation study on different decoder layers for autoregressive and causal QoR trajectory prediction. Values represents MAPE metric.**

Decoder	EPFL	OABCD	PD
MLP	5.33	17.38	17.75
MLP + multi-task	5.15	16.85	15.57
Auto-regressive LSTM	5.09	17.53	17.32
Transformer	4.73	16.57	14.65

**Inductive Setup (IP-Inductive):** In this setup, the circuits used during the training phase are different from those employed in testing. It is noteworthy that all recipes from the sample set are observed and applied to the circuits introduced to the model during training.

**Transductive Setup (Recipe-Inductive):** In the transductive setup, each circuit is exposed during training, but separate recipes are used for testing. Specifically, the set of recipes is partitioned into test and validation subsets, and all Circuits are visible during both training and testing phases, albeit with different recipes.

**4.3.1 Implementation Details and Parameter Settings.** In accordance with [10], for delay prediction, the AIG encoder uses two layers of GCN with a hidden embedding size of 32, while for area prediction, it employs 10 layers of GIN with batch normalization. Additionally, mean and max pooling were applied combined to generate embeddings for each level of AIG; hence, the dimension of the transformer decoder is set to 64. The number of levels is determined by the maximum depth of existing circuits for each dataset. Circuits with a lower depth are zero-padded to align their length. Early stopping has been utilized to report the best validation result in Table 2.

## 4.4 Results

**4.4.1 Comparison Study Result.** In Table 2, we evaluate the MAPE performance of various QoR prediction models against the baseline in multi trials across two setups for predicting delay and area. The baseline model is the architecture proposed in the OABCD paper [10]. In the IP-inductive setup, the LSOformer surpasses all existing models and outperforms the baseline by 5.74%, 4.35%, and 17.06% for the EPFL, OABCD, and PD datasets, respectively, in terms of delay prediction. For area prediction, LSOformer achieves a lower MAPE across all datasets compared to the baseline and nearly all models. However, on the OABCD dataset, the GNN-H model achieves the highest performance, demonstrating a 14% improvement over the baseline. This pattern holds in the recipe-inductive setup for both delay and area predictions across the three datasets, where LSOformer exceeds the baseline by 11.40%, 2.38%, and 12.82% for the EPFL, OABCD, and PD datasets in delay prediction, respectively.

**4.4.2 Ablation Study.** We assess the impact of the SSL auxiliary loss integrated to the training pipeline in IP-inductive setup using MAPE as evaluation metric. Similar to the benchmark SSL works [19], for the random setup, different parts of architecture are freezed to generate the lower bound of performance for SSL task. The difference between the results of random encoders and supervised models is considered the gap that the frozen model can potentially bridge in the best-case scenarios. Freezed LSOformer in Table 4, benefiting from QoR trajectory prediction, has performance near that

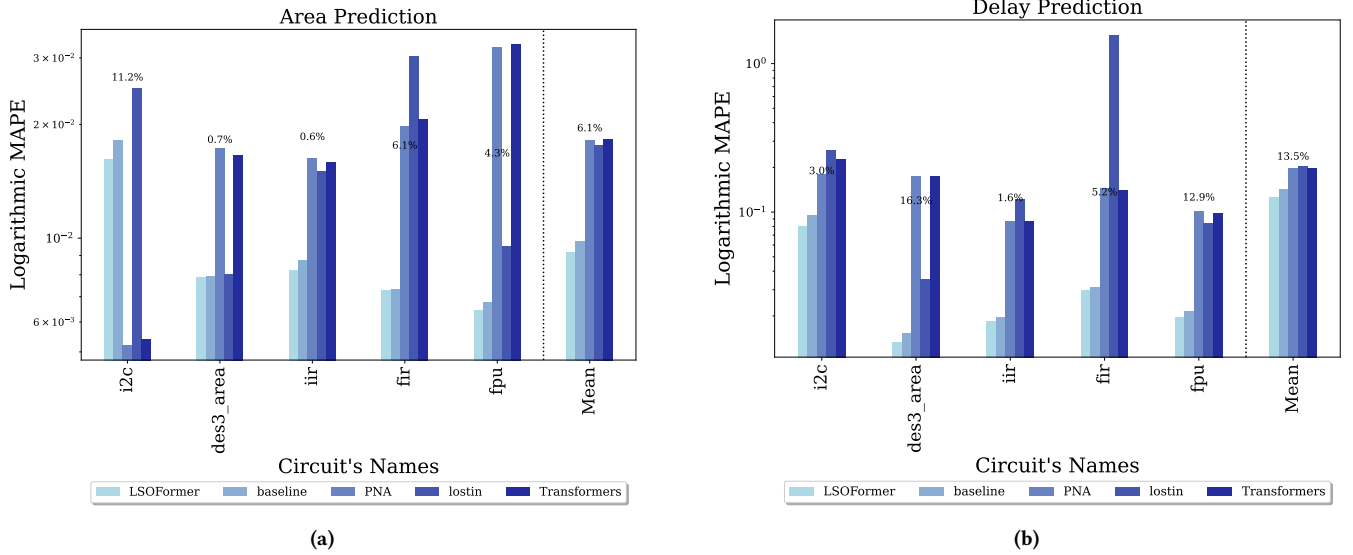


**Figure 2: Mean and circuit-wise performance comparison across test circuits for Area (a) and Delay (b).**

of the supervised LSOformer and shows better results compared to the baseline, although it has not trained on final QoR.

Table 5 details an ablation study on the integration of transformer architecture and SSL auxiliary tasks within the LSOformer model. It examines the impact of combining QoR trajectory predictions with various architectures. The results indicate that integrating our proposed architecture with the SSL task significantly improves performance over the baseline and other configurations. Conversely, removing the SSL component results in performance that does not meet the baseline levels. Additionally, using the baseline architecture for QoR trajectory prediction shows limited improvement on the EPFL dataset and a decline on the OABCD dataset, underscoring the critical role of the SSL task in enhancing the efficacy of our transformer architecture. This suggests that with ample data, the transformer decoder is particularly effective for the LSO task.

The effects of varying the embedding fusion and decoder configurations using different sequence decoders are explored in this work. The baseline model, which uses a shared MLP to predict all QoRs from initial to final, performs worse than alternative designs. Alternatively, separate MLPs are employed for each QoR, adopting a multi-task learning approach. This configuration significantly enhances performance across all datasets compared to the baseline. Additionally, we experimented with an auto-regressive LSTM module designed to train and infer models auto-regressively, thereby introducing causality to LSTM. This model demonstrates improvements over the baseline in all datasets except for OABCD. As can be seen in Table 6, the LSOformer surpasses both the baseline and all other methods across the three datasets, affirming the efficacy of our architectural design choices.

**4.4.3 In-depth Analysis.** We assess the performance of our model on a test set in comparison to established baselines. In this configuration, the model is trained using PD datasets and primarily evaluated using OABCD and EPFL datasets. The analysis involves

a randomized execution across a predetermined set of IPs, with results illustrated in Figure 2. Each column, representing an individual IP, displays the MAPE in logarithmic scale for area and delay for each model, as shown in Figure 2a and Figure 2b, respectively. The IP names are arranged in ascending order from left to right based on the number of nodes. The final column presents the average MAPE across all IPs within the EPFL and OABCD datasets. Overall, LSOformer surpasses all competing models in this setup, affirming its dominance in the LSO task. Additionally, LSOformer demonstrates a notable improvement in area performance, approximately 6%, across all IPs. For delay, although the improvement margin is narrower, there is a consistent enhancement observed across all selected IPs. The improvement gain of LSOformer, calculated as the difference from the baseline divided by the baseline performance, is displayed above each bar. For all sampled IPs, both LSOformer and the baseline outperform other methods, except for the i2c IP, where PNA and Transformer demonstrate exceptional performance in predicting area.

## 5 CONCLUSION

This paper introduces an innovative solution to the Quality of Results (QoR) prediction for Logic Synthesis Optimization (LSO) problem. A novel architecture is enhanced and integrated with a Self-Supervised Auxiliary task, designed to forecast the intermediate metrics of designs. These metrics are equivalent to those generated following post-technology mapping at each optimization phase. Additionally, we introduce a distinctive pooling mechanism for encoding And-Inverter Graphs (AIGs), which is combined with heuristic inputs using a transformer decoder architecture to predict QoRs at each step in a causal manner. The efficacy of this architecture is validated against conventional models across three primary datasets. Additionally, we demonstrate the robust alignment of the proposed architecture with the Self-Supervised Learning (SSL) auxiliary task specifically defined for this problem.

## REFERENCES

[1] Tutu Ajayi and David Blaauw. 2019. Openroad: Toward a self-driving, open-source digital layout implementation tool chain. In *Proceedings of Government Microcircuit Applications and Critical Technology Conference*.

[2] Luca Amarú, Pierre-Emmanuel Gaillardon, and Giovanni De Micheli. 2015. The EPFL combinational benchmark suite. In *Proceedings of the 24th International Workshop on Logic & Synthesis (IWLs)*.

[3] Luca Amarú, Pierre-Emmanuel Gaillardon, and Giovanni De Micheli. 2015. Majority-inverter graph: A new paradigm for logic optimization. *IEEE Transactions on Computer-Aided Design of Integrated Circuits and Systems* 35, 5 (2015), 806–819.

[4] Luca Amarú, Patrick Vuillod, Jiong Luo, and Janet Olson. 2017. Logic optimization and synthesis: Trends and directions in industry. In *Design, Automation & Test in Europe Conference & Exhibition (DATE), 2017*. IEEE, 1303–1305.

[5] Robert Brayton and Alan Mishchenko. 2010. ABC: An academic industrial-strength verification tool. In *Computer Aided Verification: 22nd International Conference, CAV 2010, Edinburgh, UK, July 15–19, 2010. Proceedings 22*. Springer, 24–40.

[6] Robert K Brayton, Gary D Hachtel, and Alberto L Sangiovanni-Vincentelli. 1990. Multilevel logic synthesis. *Proc. IEEE* 78, 2 (1990), 264–300.

[7] Animesh B Chowdhury, Jitendra Bhandari, Luca Collini, Ramesh Karri, Benjamin Tan, and Siddharth Garg. 2023. ConVERTS: contrastively learning structurally invariant netlist representations. In *2023 ACM/IEEE 5th Workshop on Machine Learning for CAD (MLCAD)*. IEEE, 1–6.

[8] Animesh Basak Chowdhury, Marco Romanelli, Benjamin Tan, Ramesh Karri, and Siddharth Garg. 2024. Retrieval-Guided Reinforcement Learning for Boolean Circuit Minimization. *arXiv preprint arXiv:2401.12205* (2024).

[9] Animesh Basak Chowdhury, Benjamin Tan, Ryan Carey, Tushit Jain, Ramesh Karri, and Siddharth Garg. 2022. Bulls-Eye: Active Few-shot Learning Guided Logic Synthesis. *IEEE Transactions on Computer-Aided Design of Integrated Circuits and Systems* (2022).

[10] Animesh Basak Chowdhury, Benjamin Tan, Ramesh Karri, and Siddharth Garg. 2021. OpenABC-D: A large-scale dataset for machine learning guided integrated circuit synthesis. *arXiv preprint arXiv:2110.11292* (2021).

[11] Animesh B Chowdhury, Shailja Thakur, Hammond Pearce, Ramesh Karri, and Siddharth Garg. 2023. Towards the Imagenets of ML4EDA. In *2023 IEEE/ACM International Conference on Computer Aided Design (ICCAD)*. IEEE, 1–7.

[12] Chang Feng, Wenlong Lyu, Zhitang Chen, Junjie Ye, Mingxuan Yuan, and Jianye Hao. 2022. Batch sequential black-box optimization with embedding alignment cells for logic synthesis. In *Proceedings of the 41st IEEE/ACM International Conference on Computer-Aided Design*. 1–9.

[13] Amur Ghose, Vincent Zhang, Yingxue Zhang, Dong Li, Wulong Liu, and Mark Coates. 2021. Generalizable cross-graph embedding for gnn-based congestion prediction. In *2021 IEEE/ACM International Conference On Computer Aided Design (ICCAD)*. IEEE, 1–9.

[14] Antoine Grosnit, Cedric Malherbe, Rasul Tutunov, Xingchen Wan, Jun Wang, and Haitham Bou Ammar. 2022. BOiLS: Bayesian optimisation for logic synthesis. In *2022 Design, Automation & Test in Europe Conference & Exhibition (DATE)*. IEEE, 1193–1196.

[15] Abdelaal Hosny, Soheil Hashemi, Mohamed Shalan, and Sherief Reda. 2020. DRILLS: Deep reinforcement learning for logic synthesis. In *2020 25th Asia and South Pacific Design Automation Conference (ASP-DAC)*. IEEE, 581–586.

[16] Guyue Huang, Jingbo Hu, Yifan He, Jialong Liu, Mingyuan Ma, Zhaoyang Shen, Juejian Wu, Yuanfan Xu, Hengrui Zhang, Kai Zhong, et al. 2021. Machine learning for electronic design automation: A survey. *ACM Transactions on Design Automation of Electronic Systems (TODAES)* 26, 5 (2021), 1–46.

[17] Xing Li, Lei Chen, Jianfang Zhang, Shuang Wen, Weihua Sheng, Yu Huang, and Mingxuan Yuan. 2023. EffiSyn: Efficient Logic Synthesis with Dynamic Scoring and Pruning. In *2023 IEEE/ACM International Conference on Computer Aided Design (ICCAD)*. IEEE, 1–9.

[18] Yingjie Li, Ming Liu, Alan Mishchenko, and Cunxi Yu. 2023. Verilog-to-PyG-A Framework for Graph Learning and Augmentation on RTL Designs. In *2023 IEEE/ACM International Conference on Computer Aided Design (ICCAD)*. IEEE, 1–4.

[19] Yixin Liu, Ming Jin, Shirui Pan, Chuan Zhou, Yu Zheng, Feng Xia, and S Yu Philip. 2022. Graph self-supervised learning: A survey. *IEEE transactions on knowledge and data engineering* 35, 6 (2022), 5879–5900.

[20] Yuankai Luo, Veronika Thost, and Lei Shi. 2024. Transformers over Directed Acyclic Graphs. *Advances in Neural Information Processing Systems* 36 (2024).

[21] Alan Mishchenko, Satrajit Chatterjee, and Robert Brayton. 2006. DAG-aware AIG rewriting: a fresh look at combinational logic synthesis. In *Proceedings of the 43rd annual Design Automation Conference*. 532–535.

[22] Walter Lau Neto, Max Austin, Scott Temple, Luca Amaru, Xifan Tang, and Pierre-Emmanuel Gaillardon. 2019. LSOOracle: A logic synthesis framework driven by artificial intelligence. In *2019 IEEE/ACM International Conference on Computer-Aided Design (ICCAD)*. IEEE, 1–6.

[23] Yu Qian, Xuegong Zhou, Hao Zhou, and Lingli Wang. 2024. An Efficient Reinforcement Learning Based Framework for Exploring Logic Synthesis. *ACM Transactions on Design Automation of Electronic Systems* 29, 2 (2024), 1–33.

[24] Raanan Y Rohekar, Yaniv Gurwicz, and Shami Nisimov. 2024. Causal Interpretation of Self-Attention in Pre-Trained Transformers. *Advances in Neural Information Processing Systems* 36 (2024).

[25] Yu Rong, Yatao Bian, Tingyang Xu, Weiyang Xie, Ying Wei, Wenbing Huang, and Junzhou Huang. 2020. Self-supervised graph transformer on large-scale molecular data. *Advances in neural information processing systems* 33 (2020), 12559–12571.

[26] Tsutomu Sasao. 1993. *Logic synthesis and optimization*. Vol. 2. Springer.

[27] Zhengyuan Shi, Hongyang Pan, Sadaf Khan, Min Li, Yi Liu, Junhua Huang, Hui-Ling Zhen, Mingxuan Yuan, Zhufei Chu, and Qiang Xu. 2023. Deepgate2: Functionality-aware circuit representation learning. In *2023 IEEE/ACM International Conference on Computer Aided Design (ICCAD)*. IEEE, 1–9.

[28] Atefeh Sohrabizadeh, Yunsheng Bai, Yizhou Sun, and Jason Cong. 2023. Robust GNN-based representation learning for HLS. In *2023 IEEE/ACM International Conference on Computer Aided Design (ICCAD)*. IEEE, 1–9.

[29] Veronika Thost and Jie Chen. 2021. Directed acyclic graph neural networks. *arXiv preprint arXiv:2101.07965* (2021).

[30] Ashish Vaswani, Noam Shazeer, Niki Parmar, Jakob Uszkoreit, Llion Jones, Aidan N Gomez, Łukasz Kaiser, and Illia Polosukhin. 2017. Attention is all you need. *Advances in neural information processing systems* 30 (2017).

[31] Peiyu Wang, Anqi Lu, Xing Li, Junjie Ye, Lei Chen, Mingxuan Yuan, Jianye Hao, and Junchi Yan. 2023. Easymap: Improving technology mapping via exploration-enhanced heuristics and adaptive sequencing. In *2023 IEEE/ACM International Conference on Computer Aided Design (ICCAD)*. IEEE, 01–09.

[32] Ziyi Wang, Chen Bai, Zhuolun He, Guangliang Zhang, Qiang Xu, Tsung-Yi Ho, Bei Yu, and Yu Huang. 2022. Functionality matters in netlist representation learning. In *Proceedings of the 59th ACM/IEEE Design Automation Conference*. 61–66.

[33] Clifford Wolf. 2016. Yosys open synthesis suite. (2016).

[34] Lirong Wu, Haitao Lin, Cheng Tan, Zhangyang Gao, and Stan Z Li. 2021. Self-supervised learning on graphs: Contrastive, generative, or predictive. *IEEE Transactions on Knowledge and Data Engineering* 35, 4 (2021), 4216–4235.

[35] Nan Wu, Jiwon Lee, Yuan Xie, and Cong Hao. 2022. Lostin: Logic optimization via spatio-temporal information with hybrid graph models. In *2022 IEEE 33rd International Conference on Application-specific Systems, Architectures and Processors (ASAP)*. IEEE, 11–18.

[36] Nan Wu, Yuan Xie, and Cong Hao. 2022. AI-assisted Synthesis in Next Generation EDA: Promises, Challenges, and Prospects. In *2022 IEEE 40th International Conference on Computer Design (ICCD)*. IEEE, 207–214.

[37] Chenghao Yang, Yinsui Xia, and Zhufei Chu. 2022. The prediction of the quality of results in Logic Synthesis using Transformer and Graph Neural Networks. *arXiv preprint arXiv:2207.11437* (2022).

[38] Chenghao Yang, Yinsui Xia, Zhufei Chu, and Xiaojing Zha. 2022. Logic synthesis optimization sequence tuning using RL-based LSTM and graph isomorphism network. *IEEE Transactions on Circuits and Systems II: Express Briefs* 69, 8 (2022), 3600–3604.

[39] Shuwen Yang, Zhihao Yang, Dong Li, Yingxueff Zhang, Zhauguang Zhang, Guojie Song, and Jianye Hao. 2022. Versatile multi-stage graph neural network for circuit representation. *Advances in Neural Information Processing Systems* 35 (2022), 20313–20324.

[40] Haisheng Zheng, Zhuolun He, Fangzhou Liu, Zehua Pei, and Bei Yu. 2024. LSTP: A Logic Synthesis Timing Predictor. (2024).

Received 20 February 2007; revised 12 March 2009; accepted 5 June 2009